JOURNAL OF CATALYSIS 62, 140–148 (1980)

Mechanism of the Reaction of NO and NH_3 on Vanadium Oxide Catalyst in the Presence of Oxygen under the Dilute Gas Condition

MAKOTO INOMATA, AKIRA MIYAMOTO, AND YUICHI MURAKAMI

Department of Synthetic Chemistry, Faculty of Engineering, Nagoya University, Furo-cho, Chikusa-ku, Nagoya 464, Japan

Received June 13, 1979; revised September 12, 1979

The NO–NH_3 reaction on vanadium oxide catalyst under the dilute gas condition was markedly accelerated by the addition of O_2. The oxygen species responsible for the acceleration of the reaction has been found to be the $V^{5+}{=}O$ species on the catalyst; the rate of the NO–NH_3 reaction at a given O_2 concentration was in proportion to the amount of the $V^{5+}{=}O$ species in the catalyst. On the basis of the results of the kinetics of the reaction in the presence of O_2, the adsorptions of NH_3 and NO, and the reaction of adsorbed NH_3 and gaseous NO, the mechanism of the NO–NH_3 reaction on vanadium oxide catalyst under the dilute gas condition has been established as follows: NH_3 is strongly adsorbed adjacent to $V^{5+}{=}O$ as NH_4^+ (ad), whereas, NO is hardly adsorbed on the catalyst. Then, a gaseous NO reacts with the adsorbed NH_3, i.e., NH_4^+ (ad), to form N_2, H_2O, and V–OH. The V–OH species is reoxidized to $V^{5+}{=}O$ by either gaseous O_2 or bulk $V^{5+}{=}O$ species. The rate of the NO–NH_3 reaction in the presence of O_2 has been proven to agree with that calculated by using the transition state theory together with the above-mentioned mechanism.

INTRODUCTION

Attention is focused on the catalytic reduction of nitric oxide with ammonia (the NO–NH_3 reaction) from the environmental point of view. Detailed mechanisms of the reaction have also been proposed for various catalysts, such as precious metals (*1–4*), metal oxides (*5–7*), and zeolites (*8–10*). However, these mechanisms have been mainly obtained by using the closed gas circulating reaction technique coupled with the tracer technique or infrared measurements. On the other hand, in the industrial process, the flow reaction technique is employed under the dilute gas condition. This condition is significantly different from that in the closed gas circulating reaction technique. Although the mechanisms obtained by using the closed gas circulating reaction technique give valuable information on the reaction under the dilute gas condition employed in the industrial process, when applying the mechanisms to the reaction under the dilute gas condition, care must be taken to the difference in the experimental conditions, especially when the gaseous oxygen is concerned in the reaction. This is because, for instance, it is clear from the kinetic data of Bodenstein (*11*) that the oxidation of NO by O_2 in the gas phase NO + $1/2O_2 \rightarrow NO_2$, takes place readily under the experimental condition using the closed gas circulating reaction technique, where concentrations of reactants are usually several tens Torr and the reaction time is around a few minutes or longer. On the other hand, according to the data of Bodenstein (*11*), the oxidation of NO by O_2 in the gas phase can hardly occur under the dilute gas condition where concentration of NO is lower than 1000 ppm and the residence time in the flow reactor is usually shorter than 0.1 sec.

Vanadium oxide catalyst is used in practice as one of the best catalysts for the NO–NH_3 reaction, because of its high activity at a lower temperature and of its high resistance to the poisoning by SO_x. Furthermore, under the dilute gas condition, it is well known that the rate of the reaction on vanadium oxide catalyst is much acceler-

0021-9517/80/030140-09$02.00/0

ated by the addition of oxygen (*12–14*). Concerning the mechanism of the reaction of V_2O_5, Takagi *et al.* (*7*) proposed the following mechanism by using the closed gas circulating reaction technique: NO_2 (ad), produced by the reaction $NO + 1/2O_2 \rightarrow NO_2$ (ad), reacts readily with adsorbed NH_3, i.e., NH_4^+ (ad), to form N_2 and H_2O, where (ad) refers to an adsorbed species. On the other hand, by using the pulse reaction technique, Miyamoto *et al.* (*15*) found that the rate of the $NO–NH_3$ reaction on vanadium oxides with various oxidation states increases in proportion to the amount of the $V^{5+}{=}O$ species on the catalyst. It is then evident that the oxygen species responsible for the acceleration of the reaction differs very much depending on the experimental methods. Therefore, it is of vital importance to investigate precisely the $NO–NH_3$ reaction under the dilute gas condition in order to establish the correct mechanism of the acceleration of the $NO–NH_3$ reaction by oxygen under the dilute gas condition (*16*).

In the present study, the authors investigated kinetically the details of the $NO–NH_3$ reaction under the dilute gas condition to propose the mechanism of the $NO–NH_3$ reaction in the presence of oxygen, which is applicable to the reaction in the industrial process. The validity of the mechanism was supported by the control experiments using pulse reaction technique, temperature-programmed desorption technique (TPD), and infrared *in situ* measurements.

NOMENCLATURE

A_ω	Absorbance at a given wave number, ω
C_{NO}	Concentration of NO in the gas phase, mole/cm^3, molecules/cm^3, or ppm
C_{NH_3}	Concentration of NH_3 in the gas phase, mole/cm^3, molecules/cm^3, or ppm
C_{O_2}	Concentration of O_2 in the gas phase, molecules/cm^3 or percentage
C_s	Number of $V^{5+}{=}O$ species on the surface of V_2O_5, molecules/cm^2
E	Activation energy, cal/mole
$F^{\neq}$	Partition function of the activated complex
F_A	Partition function of A species
f^A_{tr}	Translational partition function of A species
f^A_{rot}	Rotational partition function of A species
f^A_{vib}	Vibrational partition function of A species
h	Planck's constant, erg · sec
k	Reaction rate constant, cm^3/g · sec or cm/sec
k_B	Boltzmann's constant, erg/deg
R	Gas constant, cal/deg · mole
r	Reaction rate, mole/g · sec or molecules/cm^2 · sec
T	Absolute temperature, K

EXPERIMENTAL

V_2O_5 was prepared by the thermal decomposition of ammonium metavanadate in the stream of oxygen at 500°C for 3 hr. The BET surface area of the catalyst was 5.4 m^2/g. Kinetic studies were carried out with a conventional flow reactor under the dilute gas condition. Concentrations of reactants were varied ranging from 0 to 2000 ppm for both NO and NH_3, and from 0 to 3% for O_2 with helium as a balance gas. The quantity of O_2 as an impurity in NO, NH_3, or He gas was negligibly small. Reaction temperature was varied from 180 to 330°C, at which the oxidation of NH_3 was negligible. W/F was changed from 0.066 to 0.33 g-cat · hr/mole. Product components, i.e., N_2 and N_2O, were analyzed with gas chromatography. The structures of vanadium oxide catalysts in the steady states of the $NO–NH_3$ reaction at various concentrations of O_2 were measured by using the following methods: The infrared measurements of the catalysts were made with KBr disk method on a Jasco-IR-G spectrometer. The ESR spectra of V^{4+} ion were observed at X-band employing a JEOL ME 1X spectrometer to measure the quantity of V^{4+} ions in the catlaysts. The IR measurements of the adsorptions of NO and NH_3 and the reaction of both reactants were carried out *in situ*. Before the adsorptions, the disk of V_2O_5 was heated *in situ* under vacuum at 400°C for 1 hr and then oxidized by 120 Torr of oxygen at 400°C for 1 hr. The TPD apparatus for the adsorptions of NH_3 and NO was almost the same as that used by Cvetanovic and Amenomiya (*17*) and the temperature was raised at the rate of 10°C/min. The apparatus for the pulse experiments was similar to that described previously (*15, 18*).

RESULTS AND DISCUSSION

Effect of the Concentration of O_2 on the Rate of the $NO-NH_3$ Reaction

Figure 1 shows the effect of the concentration of O_2 on the steady-state rate of the $NO-NH_3$ reaction at 250°C under the dilute gas condition. The production rate of N_2 increased almost linearly with the concentration of O_2 up to 1%, while that of N_2O did not vary with the concentration of O_2. Figure 2 shows the results of the change in the conversion of NO in the $NO-NH_3$ reaction after the stoppage of O_2 gas supply. The conversion decreased gradually at both 252 and 308°C, and attained steady-state values after 60–70 hr duration of the reaction, which was exactly equal to the conversions at $C_{O_2} = 0\%$. Considering the above situation, the data shown in Fig. 1 were obtained 60–70 hr after the reaction began.

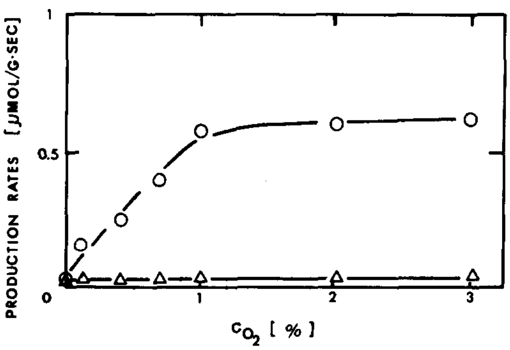

FIG. 1. Effect of O_2 concentration on the production rates of N_2 and N_2O at 250°C. Inlet concentrations of NO and NH_3 = 1000 ppm. ○, N_2. △, N_2O. W/F = 0.33 g · hr/mole.

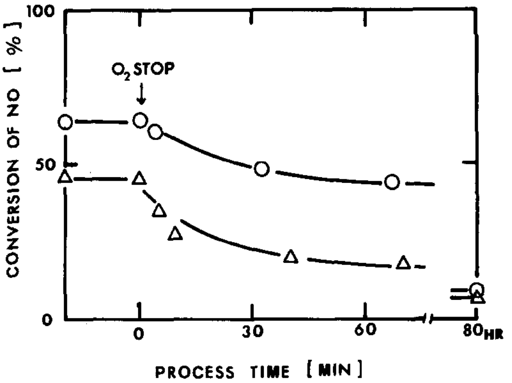

FIG. 2. Changes in the conversion of NO in the $NO-NH_3$ reaction after the stoppage of O_2 gas supply. ○, 308°C. △, 252°C. At $t < 0$ $C_{O_2} = 1.5\%$, whereas at $t \geq 0$ $C_{O_2} = 0\%$. Inlet concentrations of NO and NH_3 = 1000 ppm. W/F = 0.33 g · hr/mole.

Structure of Catalysts under the $NO-NH_3$ Reaction at Various Concentration of O_2

A catalyst in the $NO-NH_3$ steady-state reaction at a given concentration of O_2 was rapidly cooled to room temperature to measure the structure of the catalyst by using IR and ESR spectroscopies. Infrared spectra of the catalysts at various concentrations of O_2 are indicated in Fig. 3. The vanadium oxide catalysts in the steady states of the reaction above 1000 ppm of O_2 gave the absorption bands at about 1020 and 825 cm^{-1} which are assigned to the stretching vibration of $V^{5+}=O$ and the coupled vibration of $V^{5+}=O$ and V—O—V, respectively (*15, 19*). In the vanadium oxides in the steady states of the reaction below 1% of O_2, absorption bands at 990 and 910 cm^{-1} were observed. These bands are assigned to the lattice vibrations of V_2O_4 (*20*). IR spectrum of the vanadium oxide in the steady state of the $NO-NH_3$ reaction in the absence of O_2 was almost the same as that of V_2O_4. Furthermore, it is obvious from Fig. 3 that the oxidation state

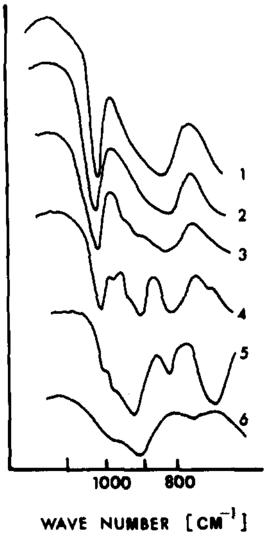

FIG. 3. Infrared spectra of vanadium oxides in the steady state $NO-NH_3$ reaction at various concentrations of O_2 at 250°C. C_{O_2} = 2.10% (1), 1.05% (2), 0.68% (3), 0.20% (4), 0.10% (5), and 0% (6).

of the catalyst above 1% of O_2 was V_2O_5. The catalyst in the steady state of the reaction below 1% of O_2 was in an oxidation state between V_2O_5 and V_2O_4 depending on the concentration of O_2. Then, in order to know the quantitative change of the amount of the $V^{5+}{=}O$ species in the catalyst with the concentration of O_2, values of $A_{1020}/(A_{1020} + A_{910})$ and $A_{825}/(A_{825} + A_{910})$ were calculated from Fig. 3, where A_ω refers to absorbance at a given wave number, ω. The relation between these relative absorbances and the concentration of O_2 in the reaction is shown in Fig. 4. The amount of $V^{5+}{=}O$ species represented by these quantities increases almost linearly with the concentration of O_2 up to 1% of O_2, and attains the constant value above 1% of O_2, where the oxidation state of the catalyst is V_2O_5. In the vanadium oxide catalysts in the steady-state reaction where O_2 concentration was below 1%, ESR signal assignable to V^{4+}(g = 1.96) was observed and the relative intensity of the signal is indicated in Fig. 5 against the concentration of O_2 in the reaction. As shown in Fig. 5, the quantity of V^{4+} in the catalyst decreased monotonically with increasing concentration of O_2 up to 1% and above this concentration it reached zero.

Oxygen Species Responsible for the Acceleration of the $NO-NH_3$ Reaction under the Dilute Gas Condition

As shown in Fig. 1, the $NO-NH_3$ reaction on vanadium oxide catalyst under the dilute gas condition is markedly accelerated by oxygen. Under the dilute gas condition using the flow technique, as mentioned above, O_2 cannot oxidize NO to NO_2 in the gas phase. According to our experiments, also, the catalytic oxidation of NO to NO_2 did not take place on vanadium oxide under the dilute gas condition. Namely, when 1000 ppm of NO and 1% of O_2 were introduced to the V_2O_5 catalyst at 300°C by using the flow technique, NO_2 was not obtained as a product. Adsorbed oxygen species can be shown not to be responsible for the acceleration of the $NO-NH_3$ reaction under the dilute gas condition as follows: No adsorbed oxygen species, such as O_2^- or O^-, was detected on V_2O_5 by either ESR or TPD measurement. Moreover, even if the catalyst surface were initially covered completely with adsorbed oxygen species, these species should be consumed by the $NO-NH_3$ reaction within 60 sec after the stoppage of O_2 gas supply and the rate of the reaction should decrease abruptly,

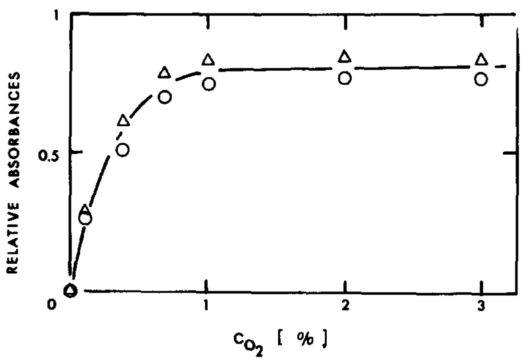

FIG. 4. Relative absorbances in infrared spectra of vanadium oxides in the steady state $NO-NH_3$ reaction at various concentrations of O_2 at 250°C. ○, $A_{1020}/(A_{1020} + A_{910})$. △, $A_{825}/(A_{824} + A_{910})$.

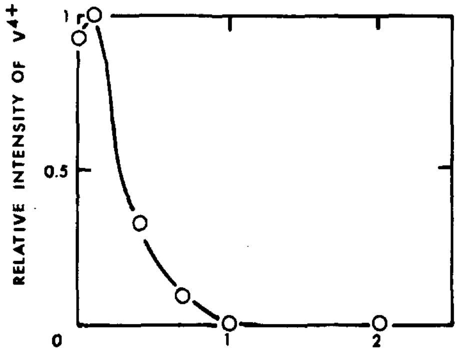

FIG. 5. Relative intensity of ESR signal at g = 1.96 for vanadium oxides in the steady state NO–NH_3 reaction at various concentrations of O_2 at 250°C.

contradictory to the experimental results shown in Fig. 2. Since the quantity of lattice oxygen of vanadium oxide catalyst is much more than that of adsorbed oxygen and the lattice oxygen of the catalyst can diffuse easily from bulk to surface, the results shown in Fig. 2 can satisfactorily be interpreted in terms of the acceleration by lattice oxygen. Furthermore, the good correlation between the data shown in Figs. 1 and 4 indicates that V^{5+}=O species on the surface of the vanadium oxide is responsible for the acceleration of the NO–NH_3 reaction under the dilute gas condition. Namely, the following reactions can be proposed:

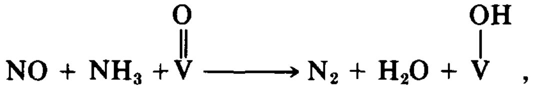

$$NO + NH_3 + \overset{\overset{\displaystyle O}{\|}}{V} \longrightarrow N_2 + H_2O + \overset{\overset{\displaystyle OH}{|}}{V}\ , \qquad (1)$$

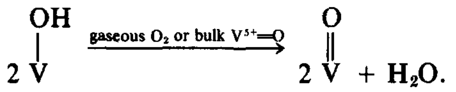

$$2\,\overset{\overset{\displaystyle OH}{|}}{V} \xrightarrow{\text{gaseous } O_2 \text{ or bulk } V^{5+}=O} 2\,\overset{\overset{\displaystyle O}{\|}}{V} + H_2O. \qquad (2)$$

According to this mechanism, when the O_2 gas supply is stopped, the V^{5+}=O species on the surface is reproduced by Reaction (2) with the expense of bulk V^{5+}=O species, followed by the formation of V^{4+} ion in bulk. Therefore, the rate of the NO–NH_3 reaction can decrease gradually after the O_2 gas supply is stopped, in accordance with the experiments shown in Fig. 2. According to the mechanism, also, the quantity of the V^{5+}=O species should decrease completely after the long duration of the NO–NH_3 reaction in the absence of gaseous O_2 and this exactly agrees with the experimental results. Namely, the quantity of V^{5+}=O species was confirmed to decrease gradually until all of the V^{5+}=O species were completely consumed (Figs. 3 and 4). Moreover, the total amount of the V^{5+}=O species consumed by the reaction was calculated to be nearly equal to the amount of oxygen necessary for the change from V_2O_5 to V_2O_4. The validity of the mechanism can also be supported by the results of the NO–NH_3 reaction on a given oxidation state of the vanadium oxide catalyst, i.e., from V_2O_4 to V_2O_5, by the pulse reaction technique (*15*). Namely, the rate of the NO–NH_3 reaction on a catalyst with a given oxidation state increased linearly with the increasing amount of V^{5+}=O species in the catalyst. This relation is similar to that derived from the data shown in Figs. 1 and 4.

Kinetics of the NO–NH_3 Reaction in the Presence and Absence of Oxygen

The kinetics of the NO–NH_3 reaction were measured under the dilute gas condition at various concentrations of O_2. When C_{O_2} was equal to 1.3%, as shown for example in Fig. 6, the rate of the NO–NH_3 reaction was first order with respect to C_{NO}, whereas it was zero order with respect to C_{NH_3}. The rate or the rate constant referred to below means that of NO disappearance.

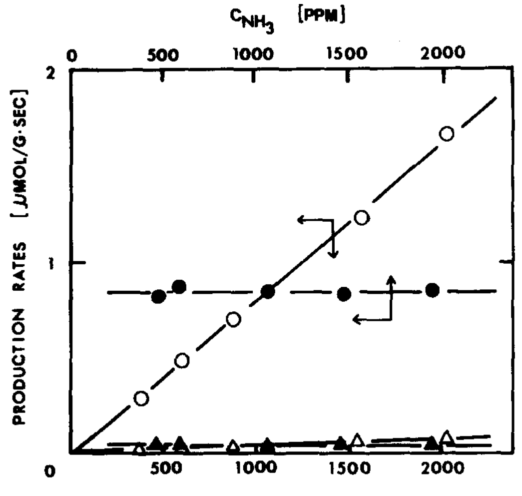

FIG. 6. Kinetics of the NO–NH$_3$ reaction on the vanadium oxide catalyst at 250°C in the presence of oxygen. ○, ●, N$_2$. △, ▲, N$_2$O. C_{O_2} = 1.3%. Open symbols: C_{NH_3} = 1000 ppm. Closed symbols: C_{NO} = 1000 ppm.

The same relation as that shown in Fig. 6 was also obtained at temperatures between 206 and 313°C. Furthermore, the rate constant of the reaction, k, at $C_{O_2} = 1.3\%$ was confirmed to satisfy the Arrhenius equation as shown in Fig. 7 with the activation energy equal to 11.6 kcal/mole. Namely, the rate of the reaction, r, at $C_{O_2} = 1.3\%$ was given by the following equation:

$$r = k\, C_{NO}^{1}\, C_{NH_3}^{0} = 1.29 \times 10^{6} \exp(-11{,}600/RT)\, C_{NO}^{1}\, C_{NH_3}^{0}\ (\text{mole/g} \cdot \text{sec}). \quad (3)$$

Taking into account the specific surface area of V$_2$O$_5$, i.e., 5.4 m^2/g-V$_2$O$_5$, the following expression is derived from Eq. (3):

$$r = 23.8 \exp(-11{,}600/RT)\, C_{NO}^{1}\, C_{NH_3}^{0}\ (\text{molecules/cm}^2 \cdot \text{sec}). \quad (4)$$

Similarly, the rate of the NO–NH$_3$ reaction in the absence of O$_2$, i.e., $C_{O_2} = 0\%$, was given by the following equation:

$$r = 32.4 \exp(-16{,}600/RT)\, C_{NO}^{1}\, C_{NH_3}^{0}\ (\text{molecules/cm}^2 \cdot \text{sec}). \quad (5)$$

From Eqs. (4) and (5), it can be noted that the difference in the rate equation between the NO–NH$_3$ reaction in the presence of O$_2$ and that in the absence of O$_2$ results not from the frequency factor but from the activation energy. Furthermore, the rate equation, i.e., Eq. (4), suggests that the NO–NH$_3$ reaction on V^{5+}=O, i.e., Reaction (1), is a reaction of a strongly adsorbed NH$_3$ and a hardly adsorbed NO, since the rate is zero order with respect to C_{NH_3} and first order with respect to C_{NO}.

Adsorptions of NH$_3$ and NO on V$_2$O$_5$

Although the rate equation shown in Eq. (4) indicates that the reaction in the presence of O$_2$ may be a reaction of a strongly adsorbed NH$_3$ and a hardly adsorbed NO with a V^{5+}=O species as the active site, this should be confirmed by the adsorption experiments of both reactants. Furthermore, the adsorbed forms of the components should be established in order to clarify the details of the reaction mechanism in the presence of O$_2$. Temperature-programmed desorption experiments showed a single desorption peak of NH$_3$, while no desorption peaks of NO were observed above room temperature, suggesting the validity of the above-mentioned inference. Furthermore, pulse chromatographic measurements of the adsorptions of NO and NH$_3$ revealed that NH$_3$ is strongly adsorbed whereas NO is hardly adsorbed

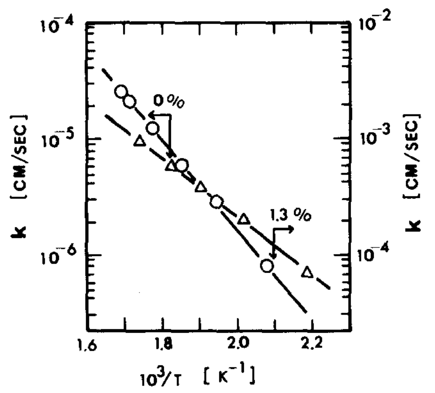

FIG. 7. Arrhenius plots of the rate constants, k, for the NO–NH$_3$ reaction in the presence and in the absence of oxygen. ○, C_{O_2} = 0%. △, C_{O_2} = 1.3%.

on V_2O_5 at 150°C (*18*). No absorption bands corresponding to NO, such as NO^+(ad), NO^-(ad), and NO_2(ad) species, were observed in the infrared spectra when NO gas was introduced onto V_2O_5 at temperature higher than room temperature. On the other hand, an adsorbed NH_3 species was clearly observed in the infrared spectra as follows: The infrared spectra of adsorbed NH_3 on V_2O_5, as shown in Fig. 8, indicate a band at 1410 cm^{-1} assignable to the deformation vibration of NH_4^+ (*7*). Consequently, it is considered that NH_3 is adsorbed on the surface of V_2O_5 as NH_4^+(ad). Here, we define the adsorption site of NH_3 (Brönsted acid site) on V_2O_5 as V_s–OH. Since the quantity of NH_3 chemically adsorbed on V_2O_5 was not affected by the oxidation or the evacuation treatment of V_2O_5 at 400–500°C before the adsorption, the adsorption site of NH_3, i.e., V_s–OH, seems to be strongly held on the surface and to be stable for the oxidation by O_2. It can be concluded that NH_3 is strongly adsorbed as NH_4^+(ad) according to the following reaction;

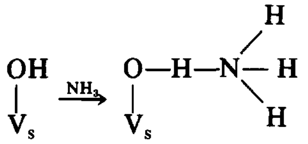

$$\underset{V_s}{\overset{OH}{|}} \xrightarrow{NH_3} \underset{V_s}{\overset{O-H-NH_3}{|}} \qquad (6)$$

while NO is hardly adsorbed on V_2O_5.

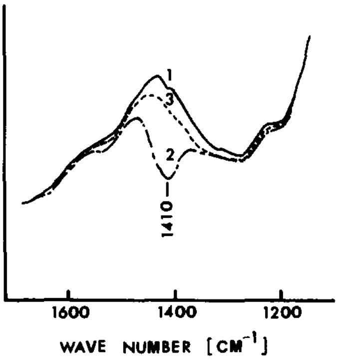

FIG. 8. Infrared spectra of adsorbed ammonia measured at room temperature before and after the reaction with NO. (1) Background. (2) After the adsorption of NH_3(60 Torr) followed by the evacuation for 30 min at room temperature. (3) After the reaction with NO(45 Torr) for 15 min at 100°C.

Reaction of Adsorbed NH_3 with Gaseous NO

As mentioned above, NH_3 is strongly adsorbed on V_2O_5 as NH_4^+(ad). When NO gas was introduced onto the catalyst preadsorbed with NH_3, the infrared band corresponding to NH_4^+(ad) disappeared at 100°C and above, as shown in Fig. 8. Furthermore, the pulse experiments indicated that the introduction of NO pulse to V_2O_5 preadsorbed with NH_3 selectively produces N_2 and H_2O at 100°C and above. Moreover, when NO gas (1000 ppm) was introduced onto the V_2O_5 catalyst treated with NH_3 (1000 ppm) using the flow reactor at 259 or 274°C, a considerable amount of N_2, i.,e., 3.8×10^{14} molecules/cm^2-V_2O_5, was produced. On the other hand, when NH_3 gas (1000 ppm) was introduced onto the catalyst treated with NO gas (1000 ppm) in the absence or in the presence of O_2 (1%) at 250°C, N_2 was not obtained at all as a reaction product, excluding a mechanism through a strongly adsorbed NO or NO_2 species (*7, 16*). These results indicate that the strongly adsorbed NH_3 species on V_2O_5, i.e., NH_4^+(ad), can react readily with a gaseous NO to form N_2 and H_2O, suggesting the Eley–Rideal mechanism.

Mechanism of the NO–NH_3 Reaction in the Presence of O_2 under the Dilute Gas Condition

As mentioned above, the kinetics of the NO–NH_3 reaction on vanadium oxide catalyst in the presence of O_2 suggests that the reaction on V_2O_5 is a reaction of strongly adsorbed NH_3 and hardly adsorbed NO. The infrared, TPD, and pulse experiments on the adsorptions of both NH_3 and NO, and on the reaction of both components support the mechanism, and, furthermore, indicate that the strongly adsorbed NH_3 species is an NH_4^+(ad) adsorbed on V_s–OH site on the catalyst. Moreover, as indicated in Reaction (1), $V^{5+}{=}O$ species on the surface of the catalyst plays an essential role as the active site for the reaction in the presence of O_2. Therefore, a further detailed mechanism of Reaction (1) can be proposed as shown in Fig. 9 [Reactions (7) and (8) are defined in Fig. 9]. Namely, at first, NH_3 is strongly adsorbed adjacent to $V^{5+}{=}O$ as NH_4^+(ad), according to Reaction (7). Then, a gaseous NO reacts with the absorbed NH_3 to form N_2, H_2O, and V–OH, according to Reaction (8), that is, the Eley–Rideal mechanism. The V–OH species produced by Reaction (8) can be reoxidized to $V^{5+}{=}O$ by either gaseous O_2 or bulk $V^{5+}{=}O$ species as indicated in Reaction (2), while the adsorption site of NH_3, i.e., V_s–OH, remains unreacted in the atmosphere of O_2 as proven above. Apparently, it seems artificial to distinguish between V_s–OH and V–OH species on the surface. Taking into consideration the crystal structure of V_2O_5 (*21*), however, the difference in behaviors of both V–OH and V_s–OH species can reasonably be understood as follows: If V_s–OH species is assumed to be a site such as Species II in Fig. 10, the V_s–OH species cannot be oxidized to $V^{5+}{=}O$ from the structural point of view, whereas, $V^{5+}{=}O$ species, i.e., Species I in Fig. 10, can be reduced to V–OH and the V–OH species formed can then be reoxidized to $V^{5+}{=}O$.

Application of the Transition Sate Theory to the Rate of the NO–NH_3 Reaction in the Presence of O_2

Since the rate of the NO–NH_3 reaction at $C_{O_2} = 1.3\%$ is limited by Reaction (8) in Fig. 9, the rate under this condition is formulated by using the transition state theory (*22*) coupled with the reaction model of Reaction (8) as follows:

$$r = \frac{k_B T}{h} C_s \frac{F^{\neq}}{F_{NO} F_{NH_4^+(ad)}} \exp(-E/RT)\, C_{NO}^{1}\, C_{NH_3}^{0}. \qquad (9)$$

It has been assumed in Eq. (9) that the adsorbed NH_3, i.e., NH_4^+(ad), is strongly held adjacent to $V^{5+}{=}O$ and, therefore, immobile on the surface. Thus, the translational and rotational partition functions of both the adsorbed NH_3 and the activated complex are considered to be unity. Consequently, the following relations can be obtained:

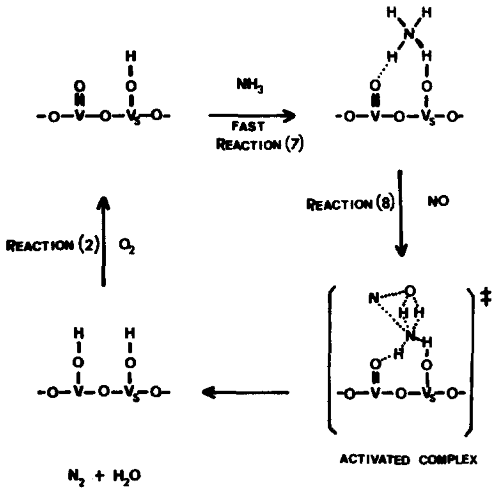

FIG. 9. Mechanism of the NO–NH_3 reaction on the vanadium oxide catalyst in the presence of oxygen.

$$F^{\neq} = f^{\neq}_{vib}, \qquad (10)$$

$$F_{NH_4^+(ad)} = 1. \qquad (11)$$

Furthermore, the number of $V^{5+}{=}O$ species on the surface, C_s, is given (*23*) by Eq. (12).

$$C_s = 2.45 \times 10^{14} \text{ molecules/cm}^2\text{-}V_2O_5. \qquad (12)$$

Substituting Eqs. (10)–(12) into Eq. (9), we get the following equation:

$$r = 0.034\, f^{\neq}_{vib} \exp(-11{,}600/RT)\, C_{NO}^{1}\, C_{NH_3}^{0} \text{ (molecules/cm}^2 \cdot \text{sec)}. \qquad (13)$$

Comparing Eq. (13) with Eq. (4), $f^{\neq}_{vib}$ is given as follows:

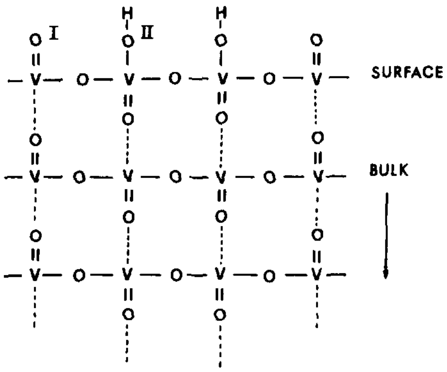

FIG. 10. Model of the surface structure of V_2O_5 catalyst. Species I, $V^{5+}{=}O$ species. Species II, $V_s{-}OH$ species.

$$f^{\neq}_{\mathrm{vib}} = 7.0 \times 10^2. \quad (14)$$

This value seems to be reasonable, since the activated complex of Reaction (8) in Fig. 9 contains many loose bonds and, according to Herschbach and Johnston (*24*), and Laidler (*22*), such a large value of $f^{\neq}_{\mathrm{vib}}$ can be expected for a loose complex comprised of many weak bonds. The alternative mechanism where NH_4^+(ad) and/or oxygen species, i.e., $V^{5+}{=}O$, can move on the surface in the initial state of Reaction (8) is rejected since the rate calculated on the basis of the latter mechanism gives a much smaller value than the experimental rate shown in Eq. (4).

As shown in Eq. (5), the rate equation of the NO–NH_3 reaction in the absence of O_2 is almost the same as that in the presence of O_2, that is, Eq. (4), except the activation energy (16.6 kcal/mole) higher than that in the presence of O_2 (11.6 kcal/mole). This gives an important suggestion on the mechanism of the reaction in the absence of O_2. Since the NO–NH_3 reaction in the absence of O_2 is composed of several elementary steps, the detailed mechanism under the condition will be reported in a subsequent paper with additional experimental data to establish the mechanism.

REFERENCES

1. Otto, K., Shelef, M., and Kummer, J. T., *J. Phys. Chem.* **74**, 2690 (1970).
2. Otto, K., Shelef, M., and Kummer, J. T., *J. Phys. Chem.* **75**, 875 (1971).
3. Otto, K., and Shelef, M., *J. Phys. Chem.* **76**, 37 (1972).
4. Otto, K., and Shelef, M., *J. Phys. Chem.* **85**, 308 (1973).
5. Niiyama, H., Ebitani, A., and Echigoya, E., *J. Catal.* **48**, 194 (1977).
6. Niiyama, H., Ookawa, T., and Echigoya, E., *Nippon Kagaku Kaishi* **1975**, 1871.
7. Takagi, M., Kawai, T., Soma, M., Onishi, T., and Tamaru, K., *J. Catal.* **50**, 441 (1977).
8. Windhorst, K. A., and Lunsford, J. H., *J. Amer. Chem. Soc.* **97**, 1407 (1975).
9. Seiyama, T., Arakawa, T., Matsuda, T., Takita, Y., and Yamazoe, N., *J. Catal.* **48**, 1 (1977).
10. Mizumoto, M., Yamazoe, N., and Seiyama, T., *J. Catal.* **55**, 119 (1978).
11. Bodenstein, M., *Z. Elektrochem.* **24**, 183 (1918).
12. Todo, N., Kurita, M., Hagiwara, H., Ueno, H., and Sato, T., Preprints of Papers for the Japan-USA Seminar on Catalytic NO_x Reactions, 3-1 (1975).
13. Bauerle, G. L., Wu, S. C., and Nobe, K., *Ind. Eng. Chem. Prod. Res. Dev.* **14**, 268 (1975).
14. Bauerle, G. L., Wu, S. C., and Nobe, K., *Ind. Eng. Chem. Prod. Res. Dev.* **17**, 117 (1978).
15. Miyamoto, A., Yamazaki, Y., and Murakami, Y., *Nippon Kagaku Kaishi* **1977**, 619.
16. Miyamoto, A., Inomata, M., Yamazaki, Y., and Murakami, Y., *J. Catal.* **57**, 526 (1979).
17. Cvetanovic, R. J., and Amenomiya, Y., *Adv. Catal.* **17**, 103 (1967).
18. Miyamoto, A., Yamazaki, Y., Hattori, T., and Murakami, Y., unpublished data.
19. Yoshida, S., *Shokubai* **10**, 90 (1968).
20. Frederickson, L. D., and Hansen, D. M., *Anal. Chem.* **35**, 818 (1963).
21. Byström, A., Wilhelmi, K. A., and Brotzen, O., *Acta Chem. Scand.* **4**, 1119 (1950).
22. Laidler, K. J., *in* "Catalysis" (P. H. Emmett, Ed.), Vol. 1, Chapt. 5. Reinhold, New York, 1954.
23. Miyamoto, A., Yamazaki, Y., Inomata, M., and Murakami, Y., *Chem. Lett.* **1978**, 1355.
24. Herschbach, D. R., and Johnston, H. S., *J. Chem. Phys.* **25**, 736 (1956).